

Natural zinc ribbon HNH endonucleases and engineered zinc finger nicking endonuclease

Shuang-yong Xu^{1,*} and Yogesh K. Gupta²

¹New England Biolabs, Inc., Research Department, 240 County Road, Ipswich, MA 01938 and ²Department of Structural and Chemical Biology, Mount Sinai School of Medicine, Box 1677, 1425 Madison Avenue, New York, NY 10029, USA

Received July 16, 2012; Revised October 4, 2012; Accepted October 8, 2012

ABSTRACT

Many bacteriophage and prophage genomes encode an HNH endonuclease (HNHE) next to their cohesive end site and terminase genes. The HNH catalytic domain contains the conserved catalytic residues His-Asn-His and a zinc-binding site [CxxC]₂. An additional zinc ribbon (ZR) domain with one to two zinc-binding sites ([CxxxxC], [CxxxxH], [CxxxC], [HxxxH], [CxxC] or [CxxH]) is frequently found at the N-terminus or C-terminus of the HNHE or a ZR domain protein (ZRP) located adjacent to the HNHE. We expressed and purified 10 such HNHEs and characterized their cleavage sites. These HNHEs are site-specific and strand-specific nicking endonucleases (NEase or nickase) with 3- to 7-bp specificities. A minimal HNH nicking domain of 76 amino acid residues was identified from *Bacillus* phage γ HNHE and subsequently fused to a zinc finger protein to generate a chimeric NEase with a new specificity (12–13 bp). The identification of a large pool of previously unknown natural NEases and engineered NEases provides more 'tools' for DNA manipulation and molecular diagnostics. The small modular HNH nicking domain can be used to generate rare NEases applicable to targeted genome editing. In addition, the engineered ZF nickase is useful for evaluation of off-target sites *in vitro* before performing cell-based gene modification.

INTRODUCTION

A large number of restriction endonucleases (REases) have been found in bacteria and viruses and are widely used in recombinant DNA technology (1–5). In contrast, relatively few natural nicking endonucleases (NEases or nickase), which introduce single-strand breaks in double-stranded DNA (dsDNA), have been discovered (3,6–8). NEases were engineered from type IIS REases

by mutating one of the two catalytic sites or disrupting the dimerization domain (9–11), by alteration of binding specificity of a type IIP REase (12) or by combining a DNA binding-deficient and catalytic-proficient FokI subunit with a DNA binding-proficient and catalytically inert FokI subunit (13). Naturally occurring nicking enzymes may be found as part of heterodimeric REases or as stand-alone enzymes. One important group of natural NEases are replication initiation proteins that specifically nick the viral genome or conjugative plasmid during phage DNA replication or conjugative plasmid transfer such as gpII of ϕ 1 phage (14) and *Salmonella typhimurium* relaxase encoded by plasmid pCU1 (15). Another group of natural NEases are homing nicking endonucleases that play a role in gene conversion (insertion of intron and intron-encoded homing endonuclease into an intron-less allele) [reviewed in (16–18)]. Artificial zinc finger nuclease (ZFN)-based nicking enzymes (ZF nickases) have been constructed by fusion of three to four ZF arrays with FokI cleavage domains, one catalytic proficient (FokIR⁺) and the other catalytic deficient (FokIR⁻). Transient heterodimer formation by R⁺/R⁻ cleavage domains upon binding to the target sites with a 5- to 6-bp spacer leads to DNA nicking which stimulates targeted gene disruption or gene addition. Such nick-induced gene targeting displays a low frequency of insertion or deletion, in sharp contrast to the non-homologous end-joining process that follows a dsDNA break and repair response (19–21). Thus, it is desirable to use ZF nickases to introduce nicks to initiate a DNA repair response that results in homology-directed recombination (HDR) for genome editing and targeted gene correction.

In addition to the ZF nickases used in genome editing, a nicking variant was engineered from I-AniI homing endonuclease (HEase) and its utility was demonstrated in nick-induced gene correction via HDR in human cells (22). Furthermore, it was shown that an I-AniI nicking variant induces homologous recombination with both plasmid and adeno-associated virus (AAV) vector templates and the nicking variant alleviates the *in vivo* toxicity problem conferred by the dsDNA cleaving

*To whom correspondence should be addressed. Tel: +1 978 380 7287; Fax: +1 978 921 1350; Email: xus@neb.com

enzyme (23). A strand-specific nicking variant has also been isolated from I-SceI HEase (24). The inherent disadvantage of using HEases in genome editing is that most of the HEases studied so far tolerate degenerate sequences, and off-target sites with a few base pair mismatches are also cleaved (25,26). ZF recombinases (ZFRs) have also been constructed by fusion of ZF arrays with Tyr or Ser recombinase for ZFR-mediated integration of the donor plasmid in mammalian genomes and site-specific recombination in a bacterial genome (27,28).

The HNH superfamily nucleases include HEases, REases, structure-specific endonucleases, non-specific nucleases, CRISPR-associated protein Cas9 (CRISPR, clustered regularly interspaced short palindromic repeat) and DNA repair enzymes. The invariant His residue in the conserved motif HNH (sometimes found as HNK or HNN) serves as the general base that activates a water molecule for a nucleophilic attack on the sugar phosphate backbone of nucleic acids. We recently investigated the restriction-modification (R-M) systems in the sequenced genome *Bacillus cereus* ATCC 10978 (GenBank: AE017194) and found a prophage-encoded multi-specificity C5 methyltransferase (MTase) and a ParB-MTase fusion protein with non-specific DNA nicking activity (29). In the vicinity of the prophage-encoded C5 MTase, three genes were predicted to encode DNA-cleaving enzymes (genes in the order of Vrr_Nuclease, DNA Integrase, HNH endonuclease (HNHE), Terminase S subunit, ParB-MTase, C5 MTase). Here, we report the DNA nicking activity of the *Bacillus cereus* HNHE. In addition, we identified and characterized nine HNHE homologs and their nicking sites. We defined a minimal nicking domain of 76 amino acids (aa) from phage γ HNHE and fused it to the zinc finger protein (ZFP) (Zif268) to generate a rare nicking enzyme with 12- to 13-bp specificity. Furthermore, we examined a number of off-target sites in λ DNA for the engineered NEase. The significance and possible biological function of this large family of strand-specific DNA NEases is discussed.

MATERIALS AND METHODS

Cloning and enzyme purification

Restriction and modification enzymes, cloning/expression vectors and chitin beads were provided by NEB. Synthetic genes encoding HNHEs with optimized *Escherichia coli* expression codons were purchased from IDT and subcloned into pTYB1 (NdeI-XhoI insert). To construct Zif268 and N. ϕ Gamma fusion, a DNA fragment encoding the minimal N. ϕ Gamma catalytic domain (F5, 76 aa) flanked by NheI and XhoI sites was inserted into pTYB1. The Zif268-encoding PCR fragment flanked by NdeI and NheI sites was inserted into the pTYB1-N. ϕ Gamma (F5). In this way, the reverse primer with a variable length of linker can be inserted between the ZF domain and the N. ϕ Gamma catalytic domain F5. IPTG induction of the intein-chitin-binding protein-HNHE fusions was carried out at 16°C overnight by addition of 0.3 mM IPTG to late-log-phase cells. Standard chitin column protein

purification procedure was followed as recommended by the supplier. HNHEs were further purified from HiTrap Heparin HP columns (5 ml) on an AKTA FPLC purification system (GE Healthcare) and stored at -20°C in a storage buffer (50 mM KCl, 10 mM Tris-HCl, 10 mM DTT, 50% glycerol).

Structural modeling of Zif268::N. ϕ Gamma fusion endonuclease

The model of N. ϕ Gamma endonuclease domain was obtained using program I-TASSER (30). The duplex DNA was built and modeled together with Zif268 (pdb id; 1aay) and N. ϕ Gamma endonuclease domains using program Coot (31).

RESULTS

Identification of HNHE N.BceSVIII from *B. cereus* and its homologs

The small predicted HNHE (121 aa) found in *B. cereus* ATCC 10987 (Supplementary Figure S1A) was expressed in *E. coli* using the IMPACT protein expression system (Supplementary Figure S1B). After purification, the protein displayed low DNA nicking activity in Mg⁺⁺ buffer and robust activity in Mn⁺⁺ buffer (data not shown) and was subsequently named N.BceSVIII. It is partially active in reaction buffers with Co⁺⁺ and is completely inhibited by addition of ethylenediaminetetraacetic acid (EDTA) (data not shown). Run-off DNA sequencing of the cleavage products indicates that N.BceSVIII cuts frequently with the recognition sequence of 5' S↓RT 3' (S = C/G, R = A/G) (Supplementary Figure S1C and D). We will use a downward pointing arrow to indicate nicking of the strand shown and an upward pointing arrow to indicate nicking of the complementary strand, following accepted nomenclature (32).

A BlastP search of the GenBank NR database using the N.BceSVIII aa sequence as a query revealed over 200 related HNHEs, all similarly small (95 to ~300 aa) and predominantly encoded by phage and prophage. These HNHE homologs can be divided into four major groups. Group 1 contains one to two zinc-binding sites with two to four zinc ribbons (ZRs) each with the motif [CxxxH], [CxxxH], [CxxxH], [HxxxH], [CxxH] or [CxxC] at the N-terminus, and the HNHE catalytic domain with one zinc-binding site with the motif [CxxC]₂ located at the C-terminus (each zinc ion is presumably coordinated by a tetrahedral geometry and thus requires two ZRs). Group 2 reverses the domain organization of the Group 1 enzymes. Group 3 lacks the N-terminal zinc-binding region of Group 1 and contains only one zinc-binding site in the HNHE catalytic domain. A non-specific HNHE (gp74) with the Group 3 domain architecture has been characterized recently from a λ -related phage HK97 (33). Group 4 HNHEs are similar to Groups 1 and 2, but located side-by-side with another ZR domain protein (ZRP) either immediate upstream or downstream. Some Group 4 enzymes are fused to the adjacent ZRP (see, e.g. Bth193 HNHE below, which has four putative zinc-binding sites). Some putative HNHEs carry additional functional domains such as a

5mC-recognition domain (MspJI family, McrA family) (34) (S.-Y. Xu, S. H. Chan and Y. Zheng, unpublished results), an NTPase domain (AAA superfamily, Walker motif A), a metalloprotease (MPN) domain or a domain of unknown function such as DUF222 (pfam02720). This report focuses on HNHEs in Groups 1, 2 and 4.

Characterization of *Bacillus anthracis* phage γ HNHE nickase

One HNHE homolog (accession YP_338236, 127 aa) from Group 1 was found in the genome of *B. anthracis* phage γ (accession NC_007458) (35), and which we will refer to as phage γ HNHE (N. ϕ Gamma or N.phiGamma). Its secondary structure as predicted by the Phyre server is shown in Supplementary Figure S2A (36). A synthetic gene was expressed in *E. coli* and the gene product purified by chromatography through two columns (Figure 1A). N. ϕ Gamma is active in the presence of Mg⁺⁺, Mn⁺⁺ or Co⁺⁺, partially active in the presence of Ca⁺⁺, Ni⁺⁺ or Zn⁺⁺ and inactive in the presence of EDTA (Figure 1B). Run-off sequencing of the cleavage products indicates that N. ϕ Gamma nicks predominantly at CG \downarrow GT sites in the presence of Mg⁺⁺ (Figure 1C and D). A small amount of linear DNA was also detected in Mg⁺⁺ buffer, most likely due to the nicking of two closely positioned sites on opposite strands. The sequence specificity is reduced to 2–3 bp recognition in Mn⁺⁺ buffer as determined by run-off sequencing of the cleavage products (data not shown). Using an independent method, we digested bacteriophage λ DNA in the presence of Mn⁺⁺ and cloned digestion products after performing a blunting reaction. Sequencing of the cloned fragments also revealed a relaxed specificity with nicking occurring at sites with one to two mismatches relative to the cognate site (data not shown).

Heat treatment of \sim 5 U of N. ϕ Gamma at 80°C for 20 min completely abolished its activity, whereas treatment at lower temperatures (55–75°C) resulted in only partial loss of nicking activity. Furthermore, treatment at 80°C for only 10 min was not sufficient for complete inactivation (data not shown).

Mapping the minimally functional nicking domain in N. ϕ Gamma

Catalytic domains of several type IIS REases including FokI, BmrI and BpuJI when cloned and purified in absence of the DNA binding domains have been shown to display non-specific nuclease activity (37–39). To test whether the N. ϕ Gamma catalytic domain (the HNHE domain) displays a similar non-specific activity in absence of the ZR domain, we deleted 66 aa (Δ 66 aa) residues from the N-terminus of the wild-type (wt) enzyme, resulting in a mutant containing only the 61 C-terminal aa residues (F6). Additional deletion mutants were also constructed, removing 22 aa (F3), 43 aa (F4) and 51 aa (F5) from the N-terminus, respectively (Supplementary Figure S2A). The deletion variants were purified and their nicking activity was assayed in Mg⁺⁺ or Mn⁺⁺ buffer. Truncated mutants F3 and F4 displayed slightly lower activity in Mn⁺⁺ buffers compared with the full-length enzyme. Mutant F5 showed nicking

activity in Mn⁺⁺ buffer and low activity in Mg⁺⁺ buffer (Supplementary Figure S2B and C), and mutant F6 has minimal nicking activity in Mg⁺⁺ or Mn⁺⁺ buffers. The nicking specificities of F4 and F5 are nearly identical: both deletion variants nick the cognate sites (CG \downarrow GT) or variations thereof with one base mismatch (F5 ‘star’ sites CG \downarrow GG, CG \downarrow GC, CA \downarrow GT or CG \downarrow AT; data not shown). It was concluded that the 61-aa C-terminal HNHE domain is not sufficient to constitute an active endonuclease activity. The smaller deletion variant F5 (76 aa in length) possesses the necessary elements for a sequence-specific NEase despite its lower activity and relaxed specificity (also see N. ϕ Gamma-F5 and Zif268 fusion below).

Enzyme concentration dependence in nicking reactions, DNA nicking kinetics in a time course by N. ϕ Gamma and flanking sequence effect on nicking efficiency

Partially purified N. ϕ Gamma and a deletion variant F3 were used to nick pBR322 DNA. At low enzyme concentration, supercoiled DNA was converted to nicked circular form. At high enzyme concentration (2–4 \times), however, a small fraction of DNA was converted to linear form, probably generated from nicks introduced on the opposite strands at adjacent sites (Supplementary Figure S2D). Supplementary Figure S2E shows a time course in N. ϕ Gamma-mediated nicking reactions. The substrate DNA (pBR322) was incubated with diluted N. ϕ Gamma from 2 min to 2 h in a limited digestion. Supercoiled DNA was partially converted to nicked circular DNA in the time period. No linear DNA was detected due to the limited digestion. In order to examine the nicking efficiency of various ACCG sites in pBR322, the DNA substrate was incubated with purified N. ϕ Gamma at 37°C for 2 h and then subjected to run-off sequencing. Supplementary Figure S2F shows a few examples of the nicked AC \uparrow CG sites followed by A, G, C or T. Overall, the DNA sites ACCGR appeared to be nicked more efficiently than ACCGY (ACCGR > ACCGC > ACCGT) by comparing the ‘A’ peak in double peaks at the run-off sites. A quantitative nicking assay to evaluate the nicking efficiency of all possible flanking sequences (N₃N₂N₁-ACCG-N₁N₂N₃) remains to be developed.

Nicking short DNA duplex oligos by N. ϕ Gamma

DNA duplex oligos with one ACCGG site (28-mer) or two ACCGG sites (32-mer) were digested by N. ϕ Gamma at 37°C for 1 h in either Mg⁺⁺ or Mn⁺⁺ buffer and the cleavage products were resolved in a denaturing gel. Both substrates were nicked and new products were detected (data not shown). In support of this, 3’ FAM-labeled duplex oligos with one ACCGN site (N = A, G, C or T) were also nicked by N. ϕ Gamma. Supplementary Figure S2G shows the nicking results of ACCGA, ACCGG, ACCGC and ACCGT duplex oligos at four enzyme concentrations. Consistent with the nicking site efficiency in pBR322, the 28-bp short oligos with ACCGR sites were nicked more readily than ACCGY sites. The nicking reactions nearly reached completion at high enzyme concentration for ACCGR oligos, whereas partial nicking was achieved using the ACCGY

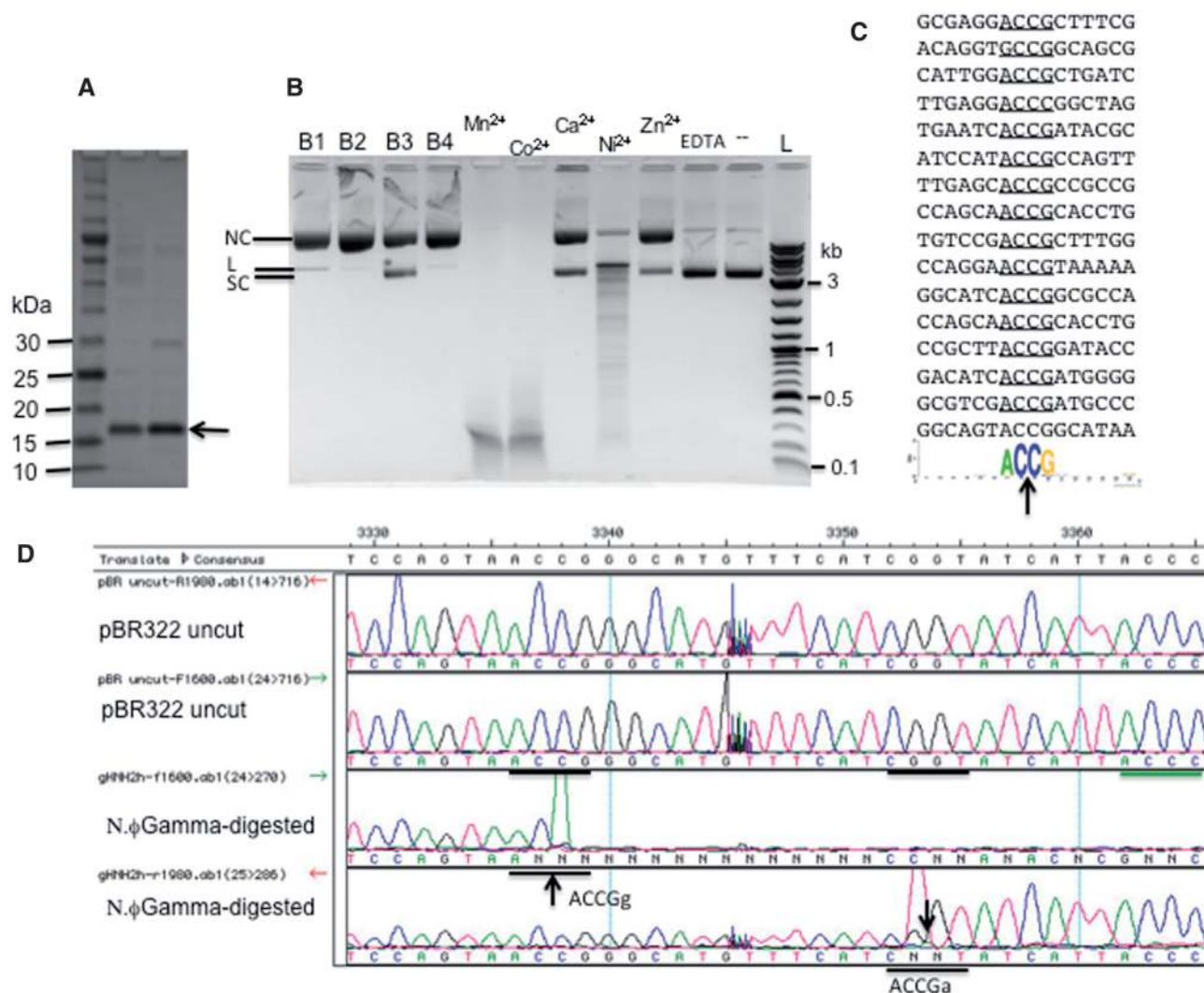


Figure 1. Characterization of phage γ HNHE (N. ϕ Gamma). (A) SDS-PAGE analysis of the partially purified N. ϕ Gamma (indicated by an arrow, predicted molecular mass of 15.5 kDa). (B) DNA cleavage assay on pBR322 in various buffers. NEB buffers B1-B4 all contain 10 mM MgCl₂. Buffer without divalent cations (10 mM Tris-HCl, pH 7.5, 50 mM NaCl, 1 mM DTT) was supplemented with metal ions (5 mM) as indicated above each lane. (C) N. ϕ Gamma nicking consensus sequence CG↓GT (AC↑CG) was compiled by WebLogo (<http://weblogo.berkeley.edu/logo.cgi>). (D) Run-off sequencing of two nicked sites. The intervening sequences have been shortened to show the two sites nicked at the opposite strands. Double peaks (A/C, A/G, A/T) indicate a nick on the template strand as the extrinsic A was added by Taq DNA polymerase by the template-independent terminal nucleotide transferase activity. Undigested pBR322 was used as a control in sequencing (top two chromatograms).

substrates. Although the exact size of the nicked products remains to be determined by running a sequencing gel at the single nucleotide resolution, it suffices to say that short DNA duplex oligos can serve as the substrates for nicking reactions by N. ϕ Gamma.

Homologs of phage gamma HNHE (N. ϕ Gamma)

A BlastP search in GenBank revealed that *Bacillus* phage Cherry and WBeta genomes encode a putative HNHE with identical aa sequence to N. ϕ Gamma (data not shown). N. ϕ Gamma also shares 99% aa sequence identity to a putative HNHE (protein ID: EJR41403, 129 aa, probably encoded by a prophage belonging to HK97 family phage) in the genome of *B. cereus* VD045 strain, and 91% aa sequence identity to a putative HNHE (protein ID: YP_001375827, 127 aa, probably encoded by a prophage similar to P27 family phage, and located next

to open reading frames (ORFs) coding for terminase small and large subunits) in the genome of *Bacillus cytotoxicus* NVH 391-98 strain. The next group of putative HNHEs from *Geobacillus* phage or prophage shares 51–56% aa sequence identity to that of N. ϕ Gamma. Because of the high aa sequence identity (similarity) among these HNHEs, it is highly likely that they are nicking enzymes with nicking site CG↓GT (AC↑CG) or minor variations of such a sequence. Consistent with this prediction, the HNHE encoded by *Geobacillus* virus E2 (N. ϕ E2), which shares 51% aa sequence identity to N. ϕ Gamma, displays the nicking specificity of CG↓GT (data not shown) (Table 1).

Lactobacillus phage Sal2 HNH nicking endonuclease

An HNHE homolog was found in the *Lactobacillus* phage Sal2 with additional aa blocks located upstream and

Table 1. Summary of DNA nicking sites by phage- or prophage-encoded HNHE and engineered chimeric nicking enzyme

Phage/prophage HNHE	No. of amino acids	Nicking site in Mg ⁺⁺ buffer	Nicking site in Mn ⁺⁺ buffer
<i>B. cereus</i> ATCC 10978 (N.BceSVIII)	121	ND (low activity)	S↓RT (AY↑S)
<i>Bacillus</i> phage γ (N.φGamma)	127	CG↓GT (<u>AC</u> ↑CG)	1-2 bp mismatches to CGGT
<i>Bacillus</i> phage 105 (N.φ105)	130	YG↓GT (R <u>AC</u> ↑CR)	ND
<i>Bacillus subtilis</i> subsp. spizizenii W23	124	BG↓GT (<u>AC</u> ↑CV)	ND
Prophage BSUW23_09635 (N.BsuW23I)			
<i>B. thuringensis</i> str T13001 (Bth193 or N.BthT13001I)	193	CSG↓GT (<u>AC</u> ↑CSG)?	SG↓GT (AC↑CS)
<i>Clostridium</i> phage phi3626 (N.φ3626)	142	BCG↓AY (RT↑CGV)	ND
<i>Geobacillus</i> virus E2 (N.φE2)	130	CG↓GT (<u>AC</u> ↑CG)	ND
<i>Lactobacillus</i> phage Sal2 (N.φSal2)	176	WNHTG↓CTC (<u>GAG</u> ↑CADNW)?	TG↓CTC (<u>GAG</u> ↑CA) or 1- to 2-bp mismatches
<i>Lactobacillus</i> phage Lrm1 (N.φLrm1)	264	ND (low activity)	HSSG↓GT (<u>AC</u> ↑CSSD)
<i>Staphylococcus aureus</i> Y74T Prophage Sap040a_009 (N.SauY74I)	119	ND (low activity)	CG↓GT, GG↓GT, TG↓GT, CG↓AT, CG↓GA
Zif268::N.φGamma F5 (chimera)	197	<u>AT</u> ↑CGN ₆ GCGTGGGCG	ND

ND, not determined. DNA single letter code, W: A/T; S: G/C; R: A/G; Y: C/T; B: C/G/T (not A); D: A/G/T (not C); V: A/C/G (not T); H: A/C/T (not G).

?, need more experimental evidence.

Underlined target sites with 4-bp variations (ACCG, ACCR, ACCV, ACCS, RCTG, AGCA, ACYG) are shared by these HNHEs.

Proposed nomenclature: HNH nicking enzymes encoded by phage: N.φ+phage name; NEases encoded by prophage or host genome (5,32).

downstream of the HNH catalytic domain (protein ID: YP_535176), which may confer additional base recognition (40). Supplementary Figure S3A shows that the two additional blocks of aa sequences (5-aa and 11-aa residues) at the N-terminus and one extra block of 32-aa residues located at the C-terminal end compared with phage N.φGamma. Phage Sal2 HNHE (N.φSal2 or N.phiSal2) was purified and used to digest pBR322. N.φSal2 shows robust nicking activity in Mn⁺⁺ buffer, which efficiently nicks DNA sites TG↓CTC (GAG↑CA) and related sites with 1- to 2-bp mismatches from the core sequence such as CG↓CTC or TG↓TTC (Figure 2A, and data not shown). Supplementary Figure S3B compiled the nicking sites (GARCA or its variants) by WebLogo using pBR322 digested in Mn⁺⁺ buffer. N.φSal2 partially nicks pBR322 in the presence of Mg⁺⁺ (data not shown). Figure 2B shows the five nicking sites, which spans 14-bp DNA with a core recognition site of GAGCA DNW (SSN₄GAGCADNW) (S, C/G; D, A/G/T, not C; W, A/T). The sixth base of the core is intolerant of a C because no GAGCAC-related sites were nicked (data not shown). In summary, N.φSal2 shows optimal nicking activity in Mn⁺⁺ buffer, nicking at TG↓CTC (GAG↑CA) or variant sites with 1- to 2-bp mismatches.

HNHE Bth193 from of *Bacillus thuringensis* strain T13001

We identified another N.φGamma homolog encoded on a prophage in the genome of *B. thuringensis* strain T13001 (protein ID: ZP_04118662). This enzyme, named as N.BthT13001I (a.k.a. Bth193 HNHE), has an additional N-terminal region relative to N.φGamma containing four ZR motifs (Supplementary Figure S4A). N.BthT13001I was expressed in *E. coli* and partially purified. It nicks DNA sequences GG↓GT or CG↓GT in Mn⁺⁺ buffer as determined by run-off sequencing (Supplementary Figure

S4B and D, data not shown). The nicking sites in pBR322 were compiled by WebLogo as SG↓GT (Supplementary Figure S4B). In Mg⁺⁺ buffer, however, N.BthT13001I recognizes and nicks DNA sites with a core sequence of CSG↓GT (AC↑CSG) (Supplementary Figure S4C). Based on the high sequence similarity with N.φGamma, we tentatively concluded that the HNH catalytic domain recognizes the SGGT sequence, and the additional ZRs at the N-terminus might contribute to the extra base C recognition in CSGGT.

We also tested whether the HNH catalytic domain is interchangeable between N.BthT13001I and N.φGamma. The N-terminus ZR of N.BthT13001I was fused with the 76-aa N.φGamma catalytic domain (F5) to form a chimeric protein (the arrow in Supplementary Figure S4A indicates the fusion junction). The nicking sites of the fusion NEase are nearly identical to that of N.BthT13001I, but with preference for CCG↓GT (AC↑CGG) sequence, further confirming the 'C' base recognition conferred by the extra ZRs (data not shown). We concluded that the HNH catalytic domain is readily exchangeable between Bth193 and N.φGamma and the chimeric enzyme N-N.BthT13001I::C-N.φGamma (F5) prefers CCG↓GT sites for nicking.

HNH nicking endonuclease gp54 from *Lactobacillus* phage Lrm1 and other HNHEs

In the sequenced genome of *Lactobacillus* phage Lrm1 (phage genome accession number: EU246945) (41), the last gene (gp54, protein ID: ABY84355) was annotated as a terminase S subunit. However, two other genes encoding terminase small and large subunits are located at the left arm of the phage genome (Supplementary Figure S5A). This predicted protein (gp54, 264-aa long) contains a HNH catalytic domain near the N-terminus (H₇₇-N₉₃-H₁₀₂) and a AAA-NTPase

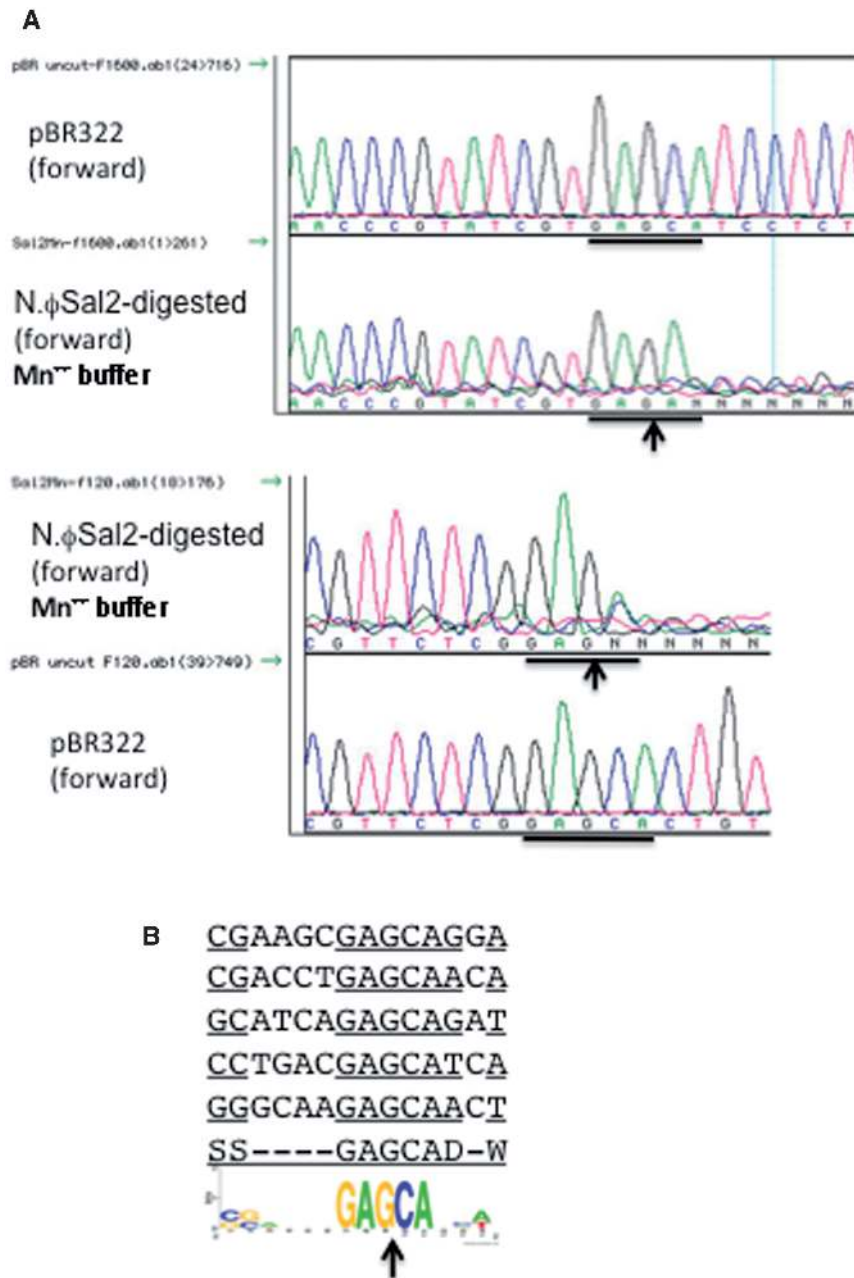


Figure 2. Characterization of phage Sal2 HNHE (N.φSal2). (A) Run-off sequencing of two nicked sites TG↓CTC (GAG↑CA) in pBR322 which was digested by N.φSal2 in Mn⁺⁺ buffer. (B) Nicking sites in pBR322 (Mg⁺⁺ buffer) compiled by WebLogo.

domain (also termed Walker A motif GxxxxGK[S/T]), but lacking the Walker B motif: h4[D/E] (h4 = four hydrophobic aa residues) at the C-terminus. In addition, the C-terminus contains a putative zinc-binding motif (2xZR [HxxxH], [RxxxH] or [HxxxD]); and seven other *Lactobacillus* phage encode close homologs carrying the 2xZR motif [HxxxH]₂ (data not shown). Phage Lrm1 HNHE (N.φLrm1 or N.philrm1) was expressed in *E. coli*, partially purified by affinity chromatography through a chitin column, and used to digest pBR322 DNA; It displays DNA nicking activity in Mn⁺⁺ buffer and low activity in Mg⁺⁺ buffer (Supplementary Figure S5B and C). Addition of NTP (ATP, GTP, CTP

or UTP) failed to stimulate N.φLrm1 nicking activity (data not shown). The partially nicked DNA was gel-purified and subjected to run-off sequencing. Supplementary Figure S5D summarizes the nicking sites as HSSG↓GT (AC↑CSSD), which resembled the nicking sites of Bth193 CSG↓GT (AC↑CSG). We do not know the function of the AAA-superfamily domain (Walker A motif) at the C-terminus of N.φLrm1 as neither NTP nor dNTP have any stimulatory effect on DNA nicking activity. This domain could serve as an accessory domain interacting with DNA or other proteins. We have not studied the interaction of this HNHE with the phage Lrm1 terminase.

We also partially purified the HNHEs from *Bacillus* phage phi105 (protein ID: ADF59184), *Geobacillus* virus E2 HNHE (GBVE2_gp070, protein ID: YP_001522898) (42), *Clostridium* phage phi3626, gp50 (protein ID: NP_612879), *Staphylococcus aureus* strain Y74T prophage, ORF Sap040a_009 (protein ID: ACZ58991) (data not shown). The nicking sites of these HNHEs are summarized in Table 1.

Construction of Zif268 and N.φGamma (F5, 76 aa) fusion nicking endonuclease

A large number of natural ZFPs have been identified in the past 25 years consisting primarily of eukaryotic transcription factors (see ZF database) (43), and additional ZFPs with high DNA binding affinity have been engineered by genetic selection or phage display (44–47). Thus, ZFPs provide a collection of DNA binding modules (arrays) ranging from 6 to 12 bp with two to four individual ZFs linked together. ZFNs have been engineered to cleave large recognition sequences 12–24 bp (48–52). Individual ZFP forms a DNA recognition module with two antiparallel β-sheets and one α-helix (ββαZn), where the second β-sheet contacts the sugar phosphate backbone and the α-helix contacts the base pairs in the DNA major groove as first revealed by the structure of the Zif268–DNA complex (53).

We next attempted the fusion of the minimal N.φGamma nicking domain (F5, 76 aa) to Zif268 (3 ZFs, 117 aa) (partial ZFP sequence of North American songbird *Vireo cassinii*, GenBank accession: protein ID: AAO84760, 210 aa) to generate the chimeric enzyme Zif268III::N.φGamma F5 (designated as ZifIII for short). Two fusion proteins were constructed, R1 fusion with 13-aa linker and R2 fusion with 3-aa linker between the two functional domains (Figure 3A). The two fusion proteins were purified to near homogeneity by chromatography (Figure 3B) and used to digest pUC19 (Figure 3C) and pUC19-Zif3 (containing a Zif268 recognition sequence GCGGGGGCG). Run-off sequencing of the nicked products indicated no apparent nicking taking place within or near the GCGGGGGCG sequence (data not shown). However, a clear nicking site was detected at AT↑CG-N₆-GCGCGGGGA (underlined base pair matching N.φGamma and Zif268 recognition sequences with a 6-bp spacer) in pUC19 and pUC19-Zif3 (nicking the opposite strand CG↓AT, data not shown). This unintended nicking site (off-target site or ‘star’ site) prompted us to design a new DNA substrate with the sequence ATCG-N₆-GCGTGGGCG. Figure 3D shows a time course of the nicking reactions of pUC derivatives carrying the cognate site and two ‘star’ sites. Figure 3E shows nicking of cognate site with enzyme dependence over fixed amount of DNA. A sharp run-off signal was detected on the ZifIII R1-digested cognate site and nicking at the ‘star’ site of the pUC backbone was strongly suppressed although the chromatogram peak is low at the ‘star’ site (Figure 3F, third sequencing run). A small fraction of the DNA was nicked on the opposite strand 2 nt apart generating a 2-base 5'-overhang (Figure 3F, first sequencing run), suggesting the reason for the small

amount of linear DNA detected in the agarose gel in Figure 3E and D. For the pUC derivative with one ‘star’ site inserted at the multiple cloning sites and the original ‘star’ site in the backbone, both sites were partially nicked (Figure 3F, fourth sequencing run). Nicking at ATCG, ACCG or ACTG sites were not detected (one undigested ATCG site is indicated by a blue line in Figure 3F, data not shown). Nicking reactions performed in high salt buffer (B3) could minimize the promiscuous nicking activity as some smearing was detected in prolonged incubation in B1, B2 and B4 (data not shown). Double-stranded breaks could be minimized by shorter digestion (<30 min) and in 150 mM NaCl (~80% supercoiled DNA converted to nicked circular in 2 h in 150 mM NaCl with minimal dsDNA breaks, data not shown). These results indicate that a ZF nickase can be constructed from a ZFP (three fingers) and the N.φGamma minimal nicking domain to create a chimera capable of nicking a 12- to 13-bp target site. Addition of two or more ZFs may further increase the nicking specificity, which is a prerequisite for applications in genome editing.

Off-target nicking sites by Zif268::N.φGamma F5

To investigate potential ‘star’ sites of ZifIII R1, λ DNA was nicked by the chimeric NEase and the digested DNA was subjected to run-off sequencing at the suspected ‘star’ sites (9- to 11-bp matches). One strong off-target nicking site was found with the sequence AC↑TG-N₆-GCCGTGGAG (CA↓GT, 2-bp matches in each ZF binding site, λ coordinate 3981, Supplementary Figure S6A). Two ‘star’ sites with the sequence AC↑CC-N₆-GCGCGGGTT (GG↓GT; 3-bp, 2-bp, 1-bp matches to ZF3, ZF2 and ZF1 sites, respectively; λ coordinate 4486) and ACTG-N₆-GCGGGGGTA (CA↓GT; 3-bp, 3-bp, 1-bp matches in ZF3, ZF2 and ZF1 sites, respectively; λ coordinate 11111) were partially nicked by the ZifIII R1 NEase (Supplementary Figure S6B, data not shown). No apparent nicking was found in the suspected ‘star’ sites listed in Supplementary Figure S6C, which contains 5- to 7-bp matches to the Zif268 binding site (data not shown). These off-target sites indicate that 2-bp matches in each ZF are likely strong ‘star’ sites. The 5- to 6-bp matches in ZF3 and ZF2 in conjunction with 1-bp match in ZF1 are probable ‘star’ sites.

DISCUSSION

The minimal HNH catalytic domain with its own sequence specificity

The HNH motif is highly conserved among the HNHEs, although in some cases the second His residue can be substituted by a Lys or Asn residue (H-N-K/N). The first conserved His residue acts as a general base to activate a water molecule for nucleophilic attack of the DNA phosphodiester bond, and the Asn orients the catalytic His residue and scissile phosphate in the correct position for DNA hydrolysis (54,55). The second His (or Lys/Asn) stabilizes the leaving group. HNH domains, which generally fold into a secondary structure described as ‘ββα-metal’, bind the DNA backbone in the minor

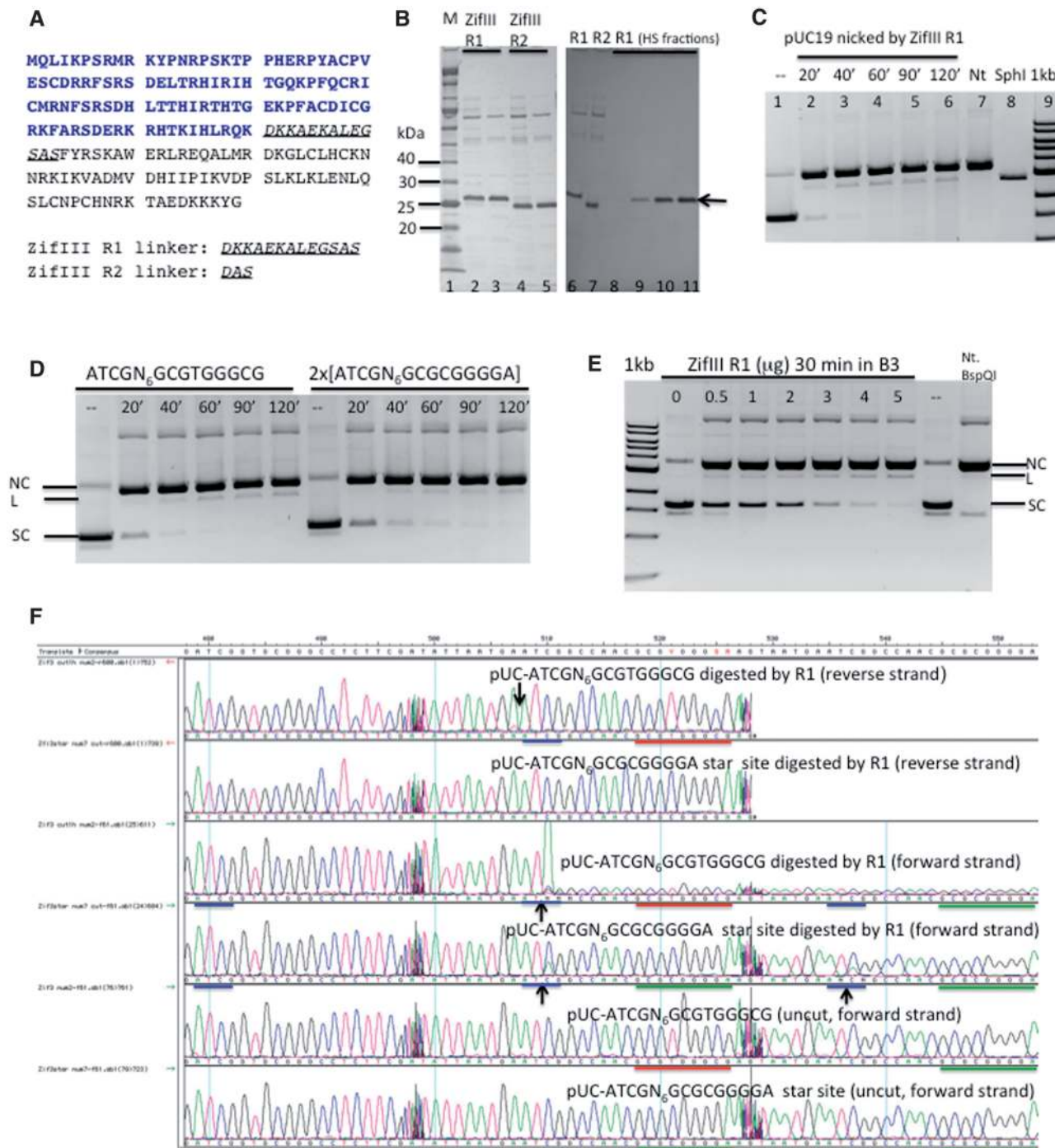


Figure 3. Characterization of Zif268::N.φGamma F5 chimeric nickase (ZifIII). (A) Amino acid sequence of the fusion HNHE (Zif268 sequence shown in blue). The sequence was derived from partial ZFP of *Vireo cassinii* (GenBank: gb AAO84760). Two fusion constructs were made, R1 with a 13-aa linker (7 aa: DKKAEKA from the native songbird Zif268) and R2 with 3-aa linker between the two functional domains. (B) SDS-PAGE analysis of purified ZifIII R1 and R2 HNHEs. Lanes 2–5, 6 and 7, purified R1 and R2 fusion proteins from chitin columns. Lanes 8–11, purified R1 fusion protein from a heparin column (HiTrap Heparin HP, 5 ml). (C) Nicked pUC19 DNA in a time course (lanes 2 and 6, 20 min to 2 h). Lanes 7 and 8, Nt.BspQI nicked and SphI-digested DNA, respectively. (D) Digestion of pUC-ATCG-N₆-Zif3(GCGTGGGCG) and pUC-ATCG-N₆-Zif3star(GCGCGGGGA) in a time course (20 min to 2 h) in Buffer 3 (100 mM NaCl). Small amount of linear DNA (<5% of total DNA) appeared after 20 min digestion. Note: there is a pre-existing ‘star’ site in pUC19 in addition to the cognate site or ‘star’ site inserted at the multiple cloning sites. (E) Digestion of pUC-ATCG-N₆-Zif3(GCGTGGGCG) by varying concentration of ZifIII R1 in NEB Buffer 3 for 30 min. The Nt.BspQI-nicked DNA was used as a marker. The slow migrating DNA in (E) and (F) is probably nicked dimer. (F) Run-off sequencing of nicked DNA (B3, 1 h, 37°C) with forward and reverse primers. Red line, Zif268 cognate site; green line: Zif268 ‘star’ site; blue line: N.φGamma site. Arrows indicate the nicking sites where double peaks appeared. SC, supercoiled; L, linear; NC, nicked circular DNA.

groove, whereas additional residues mediate sequence-specific interactions with the DNA (56). The zinc metal ion is coordinated by a tetrahedral coordinating geometry by the two ZRs [CxxC]₂ or [CxxH, CxxC] (55,57,58).

Secondary structure prediction by the Phyre server (59) revealed that the N.φGamma catalytic domain (F6, 66 aa) contains a β–β–α–α structure, as predicted from known structures of a HNHE from *Geobacter metallireducens* GS-15 (a HNHE without the extra ZR domain, pdb accession: 2qgpB, Northeast Structural Genomics Consortium target GmrR87) (A. P. Kuzin *et al.*, unpublished results) and PacI (a HNHE family REase) (57). The active deletion variant F5 (76 aa) contains an extra α-helical structure that may be involved in increased DNA-binding affinity or dimerization. It is somewhat unexpected that the deletion of the N-terminal 51-aa ZR domain does not totally abolish the specificity of N.φGamma. The deletion only weakened the activity in Mg⁺⁺ buffer and relaxed the sequence recognition. The 76-aa minimal nicking domain has been used in construction of fusion protein with ZFP. The ‘star’ sites of N.φGamma in Mn⁺⁺ are usually one base different from the cognate site AC↑CG, e.g. AT↑CG, CC↑CG, AC↑TG or GC↑CG. The off-target sites of Zif268::N.φGamma in λ DNA, however, appear to be AY↑YS (e.g. AC↑CC, AC↑TG, AT↑CG). This limited spectrum of ‘star’ sites could be result of few ‘star’ sites interrogated or lower ‘star’ activity in the high salt buffer.

We constructed two versions of Zif268::N.φGamma fusion, R1 with 13-aa linker and R2 with 3-aa linker between the ZFs and N.φGamma catalytic domains. R1 is more active than R2 in DNA nicking and both require a N₆ DNA spacer between the ZFP binding site and the N.φGamma target sequence. More Zif268 and N.φGamma fusions with variable linker length ranging from 4 to 20 aa are probably necessary to pinpoint the optimal spacing between the two functional domains. The optimal linker between ZF arrays and FokI cleavage domain appears to be 4–8 aa residues for efficient cleavage of target sites with a 6-bp spacer by ZFNs (60). To better understand how N.φGamma is likely positioned in the chimeric structure, we built three-dimensional homology-based models of DNA-bound and the apo Zif268::N.φGamma (ZifIII R1). As shown in Supplementary Figure S7, this model (monomer) adopts an elongated shape and covers roughly two turns of the DNA helix.

The ZF nickase by fusion of a ZF arrays and a FokI cleavage domain requires dimerization in order to nick the target sites, i.e. formation of a heterodimer by FokI catalytic-proficient (R⁺) and catalytic-deficient (R[−]) monomers. Similarly, TALE-FokI nickase (to be constructed and functionally tested) may also require dimer formation (TALE-FokIR⁺ and TALE-FokIR[−]) in order to nick target sites. The advantages of using a HNHE nicking domain are: (i) a single molecule construction, and thus the cost of cloning, expression and purification may be cut in half, (ii) the wide selection of natural HNHE nicking domains existing among the phage and prophage-encoded HNHE and (iii) the minimally functional nicking domain is fairly soluble in fusion with

other DNA binding partners. The disadvantage of using the N.φGamma minimal nicking domain is that it carries its own specificity. By site-directed mutagenesis, however, its specificity could be further reduced. Alternatively, one can use the nicking domain from N.BceSVIII with frequent nicking sites (S↓RT, ~2 bp) for construction of chimeric nickases. Our initial study using the HNHE nicking domain from I-HmuI indicated that it has a strong non-specific nicking activity in the absence of a DNA binding partner and therefore mutations need to be introduced to further reduce its affinity for DNA (S. H. Chan and S.-Y. Xu, unpublished results).

A ZR domain isolated from the Nob1 RNA endonuclease of the archaeon *Pyrococcus horikoshii* is sufficient to bind an RNA helix 40 of the small subunit ribosomal RNA (rRNA) (61), indicating the ZR domain has its own specificity. ZRs have been widely adopted by other nucleases and DNA/RNA metabolic enzymes and transcription factors (62–65). The ZR found in McrA endonuclease, a member of the HNHE superfamily, had been studied previously by computer modeling and structure prediction (34).

Metal ion requirement of HNHEs

A few HNHEs are only active in Mn⁺⁺ or Co⁺⁺ buffers, including N.BceSVIII, *Lactobacillus* phage Lrm1 gp54 (N.φLrm1), *S. aureus* prophage ORF Sap040a_009 HNHE. N.BceSVIII and phage N.φGamma are active in a range of 1–10 mM Mn⁺⁺ tested. Gp54 of *Lactobacillus* phage Lrm1 (N.φLrm1), however, prefers a low concentration of Mn⁺⁺ (1 mM) in nicking. Thus, the optimal Mn⁺⁺ concentration supporting maximum endonuclease activity depends on the individual enzyme. The non-specific HNHE encoded by phage HK97 contains the zinc-binding motif CxxC and CxxH in the catalytic domain. No additional zinc-binding sites (ZRs) were found at the N-terminus. HK97 gp74 HNHE prefers Ni⁺⁺ as a co-factor, although lower activity was also detected in other divalent cations (33,66). HK97 gp74 HNHE also nicks plasmid DNA, but the sequence specificity of nicking sites (if any) has not been yet determined. Previously, we found HpyAV (CCTTC N₆/N₅), a member of the HNHE family REase also prefers Ni⁺⁺ for optimal endonuclease activity (67). Interestingly, the modification-dependent endonuclease Sco McrA, an HNHE family enzyme, prefers Mn⁺⁺ or Co⁺⁺ in cleaving M.Dcm-modified DNA (68).

In N.φGamma, the conserved ‘ββα–metal’ fold is expected to display a tetrahedral coordination of a Zn ion for structural folding and an Mg⁺⁺/Mn⁺⁺ divalent cation for catalytic function. The magnesium concentration is estimated to be ~100 mM in actively growing *E. coli* cells, although most of the Mg⁺⁺ is in a bound state to nucleic acids. The Mn⁺⁺ and Zn⁺⁺ ions in *E. coli* are estimated at much lower concentration, at ~0.2–0.4 mM for Mn⁺⁺ and 0.1 mM for Zn⁺⁺ ions (cells grown in LB broth) (Bionumbers database at the web site: <http://bionumbers.hms.harvard.edu>). Based on this estimation of metal ion concentration, it is speculated that Mg⁺⁺ is more readily available for the N.φGamma

catalytic activity than Mn^{++} , which may explain the observation that most of the phage/prophage-encoded HNHE described in this work are not toxic or lethal to *E. coli*, even though some of the HNHEs have frequent nicking sites, and in the absence of companion methylase protection (or prophage gene expression may be tightly repressed). Previously, we expressed Nt.CviPII (/CCD, a frequent nickase encoded by a chlorella virus NYS-1) in *E. coli* (Nt.CviPII requires Mg^{++} for catalytic activity and belongs to the PDxExK family endonucleases). The over-expression of Nt.CviPII requires the presence of a cognate methylase for host DNA protection (7).

Off-target sites of Zif268::N.φGamma F5 fusion NEase

The N.φGamma catalytic domain F5 has its own specificity (ACCG, ACCC, ACTG or ATCG) and the Zif268 has 9-bp specificity (GCGTGGGCG or GCGGGGGCG). The fusion enzyme has the combined sequence specificities with a 6-bp spacer. Although we have not analyzed many 'star' sites of Zif268::N.φGamma F5 chimera, the following observation was made in the limited number of off-target sites in λ and pUC19 DNA. For a strong 'star' site, 2-bp matches in each finger (6-bp matches total) are better than 6-bp matches in only two fingers and 0-bp match in one finger (6-bp matches total). The 3-bp matches in ZF3, 2-bp matches in ZF2 and 1-bp match in ZF1 (6-bp matches total) appear to be a 'star' site (e.g. AC↑CG-N₆-GCGSGGGNN, ACCG can be substituted by ACCC, ATCG or ACTG). It is possible that ZF2 and ZF3 are more important than ZF1 in determination of the nicking specificity due to the proximity to the N.φGamma nicking domain or higher binding affinity to DNA. Sequencing more ZifIII R1 'star' sites is necessary to confirm this observation.

Fusion of N.φGamma F5 nicking domain to other DNA binding elements

In theory, the N.φGamma minimal nicking domain can be fused to other DNA binding proteins such as a

cleavage-deficient NotI REase. Because NotI forms a dimer, the NotI (D160N)::N.φGamma F5 fusion may nick the symmetric site AC↑CG-N_x-GCGGCCGC-N_x-CG↓GT (estimated $x = 6-12$ bp). The N.φGamma nicking domain may also be fused to a TALE effector protein, which recognizes 14-to 24-bp recognition sequences. The resulting fusion protein is expected to nick DNA at rare sites. A number of labs have developed methods for the modular construction of custom-designed TALE effector proteins and TALE nucleases (69–76). The optimal linker between TALE effector protein and the N.φGamma nicking domain needs to be tested experimentally in future work. The homeodomain fold commonly found in eukaryotic transcription factors consists of a 60-aa helix–turn–helix structure that binds to DNA or RNA. A large number of new specificities of homeodomain have been selected that can serve as the target-recognizing domain (TRD) of the fusion nicking enzyme (77). In addition, the N.φGamma nicking domain can be conjugated to LNA (locked nucleic acid) which binds to dsDNA by triple-helix formation. Similarly, the N.φGamma nicking domain can be coupled to 5mC-recognition domain such as MBD (methyl-binding domain protein) (78) or the 5mC specificity domain of MspJI-family REases, McrB, McrA, SauUSI or SRA protein, generating 5mC-specific nickases.

Possible biological function of phage and prophage-encoded HNHE

Table 2 shows the gene organization of the phage/prophage-encoded HNHE, adjacent ZR protein, terminase small and large subunits and phage portal protein. The biological function of these phage or prophage-encoded HNHE NEases is unknown. Because these NEase are located near the DNA packaging enzyme terminase, we speculate that these NEases may play a role in DNA packaging, e.g. by relieving the supercoiled tension built up during DNA translocation into the phage prohead. The nicks may stimulate

Table 2. Genes (ORFs) in proximity to the phage- or prophage-encoded HNHEs

Phage or prophage	ZR protein ^a	HNHE	ZR protein ^a	Terminase S	Terminase L	Portal protein
<i>B. cereus</i> ATCC 10978		Bce_0389		Bce_0390	_0397	_0398
<i>Bacillus</i> phage γ	γLSU_0048	γLSU_0050		γLSU_0001	_0002	_0003
<i>Bacillus</i> phage 105		phi105_00255	phi105_00260	phi105_00005	_00010	_00020
<i>Bacillus subtilis</i> subspecies spizizenii W23		Bsuw23_09635	Bsuw23_09630	Bsuw23_09625	_09620	_09610
<i>B. thuringensis</i> str T13001 (Bth193)		Bth0005_4180 ^b	unknown			
<i>B. thuringensis</i> str T13001 (Bth67)	Bth0005_53510	Bth0005_53520		Bth0005_53530	_53540	unknown
<i>Clostridium</i> phage phi3626	phi3626_p49	phi3626_p50		phi3626_p01	_p02	_p03
<i>Geobacillus</i> virus E2	GBVE2_gp069	GBVE2_gp070		GBVE2_gp001	_gp002	_gp003
<i>Lactobacillus</i> phage Sal2		LSL_279		LSL_280	_281	_282
<i>Lactobacillus</i> phage Lrm1	Lrm1_gp52	Lrm1_gp54		Lrm1_gp01	_gp02	_gp03
<i>Staphylococcus aureus</i> Y74T		Sap040A_009	Sap040A_010	Sap040A_0011	_012	_014
Prophage Sap040a_009						
Phage HK97 (AF069529)		gp74 ^c		gp1	gp2	gp3

^aThe ZR motifs of the ZR proteins located either upstream or downstream of the HNHEs contain the amino acid sequence: CxxC, CxxxH, HxxC, HxxxH, or CxxxxH;

^bThere are two HNHEs in the shot-gun genome sequences of *B. thuringensis* str T13001. The N.BthT13001I (Bth193) activity has been verified. The nicking activity of the shorter HNHE (67 aa) and the 110-aa ZR protein is unknown;

^cThe gp74 HNHE encoded by phage HK97 contains the zinc-binding motif CxxC and CxxH. Gp74 has nicking activity on plasmids (in Ni^{++} buffer).

homologous recombination and enhance gene conversion of HNHE-minus incoming phage to HNHE-plus phage, which may also occur during mixed infection. HEases make dsDNA breaks in alleles that are homologous to the endonuclease gene but lack the intron or intein element, which encodes the gene for the HEase. One example of HNH NEase-stimulated *trans*-homing was reported previously: an HNH nicking enzyme (mobE) encoded by T4 phage introduces a strand-specific nick in the non-coding strand of the *nrdB* gene of a related phage T2. MobE promotes the mobility of the neighboring non-functional homing endonuclease I-TevIII, which was encoded within a Group I intron interrupting the *nrdB* gene of phage T4 (79). In this case, the nicking enzyme functions as a ‘helper’ HEase. The HNH nicking enzymes may play a role in the lysogenic life cycle of phage. It was proposed that phage HK97 HNHE, gp74 generated dsDNA breaks (or ssDNA nicks in certain metal ions), thereby initiating bacterial SOS repair response that allows for homologous recombination at the cleavage site to occur, resulting in integration of the phage genome (66). Another possibility yet to be ruled out is introduction of dsDNA breaks by HNH nicking endonuclease in conjunction with another nickase such as ParB homologs or Vrr_nuc domain endonucleases, which together function as restriction enzymes to restrict invading DNA.

We have not studied the function of the ZRP located next to the HNHE except for the Bth193 HNHE (N.BthT13001I), which is a fusion of ZRP to HNHE with four putative zinc-binding sites (8xZRS). The adjacent ZRP could serve as the transcription regulator of the HNHE gene or as a mini-specificity subunit that could interact with the HNHE and further extend the sequence specificity. Experiments are in progress to express and purify these small ZRPs to elucidate their function and to construct chimeric fusion NEases from existing HNHEs by domain swapping.

SUPPLEMENTARY DATA

Supplementary Data are available at NAR Online: Supplementary Methods and Supplementary Figures 1–7.

ACKNOWLEDGEMENTS

We thank Richard Roberts, Bill Jack, Siu-Hong Chan, Jim Samuelson, Ted Davis and Brian Anton for critical reading of the manuscript; Nancy Badger and Barton Slatko in DNA sequencing core lab for sequencing; Siu-Hong Chan for running the molecular size exclusion column; Rebecca Nugent and Geoff Wilson for discussion; Don Comb for general interest in engineering genome-editing reagents; Jim Ellard for support.

FUNDING

Funding for open access charge: New England Biolabs, Inc.

Conflict of interest statement. Some nicking enzymes described in this paper may become commercial products.

REFERENCES

- Smith,H.O. (1974) Restriction endonuclease from *Hemophilus influenzae* Rd. *Methods Mol. Biol.*, **7**, 71–85.
- Wilson,G.G. and Murray,N.E. (1991) Restriction and modification systems. *Ann. Rev. Genet.*, **25**, 585–627.
- Van Etten,J.L., Xia,Y., Burbank,D.E. and Narva,K.E. (1988) *Chlorella* viruses code for restriction and modification enzymes. *Gene*, **74**, 113–115.
- Pingoud,A., Alves,J. and Geiger,R. (1993) Restriction enzymes. *Methods Mol. Biol.*, **16**, 107–200.
- Roberts,R.J., Vincze,T., Posfai,J. and Macelis,D. (2010) REBASE—a database for DNA restriction and modification: enzymes, genes and genomes. *Nucleic Acids Res.*, **38**, D234–D236.
- Xu,S.Y., Zhu,Z., Zhang,P., Chan,S.H., Samuelson,J.C., Xiao,J., Ingalls,D. and Wilson,G.G. (2007) Discovery of natural nicking endonucleases Nb.BsrDI and Nb.BtsI and engineering of top-strand nicking variants from BsrDI and BtsI. *Nucleic Acids Res.*, **35**, 4608–4618.
- Chan,S.H., Zhu,Z., Van Etten,J.L. and Xu,S.Y. (2004) Cloning of CviPII nicking and modification system from *Chlorella* virus NYS-1 and application of Nt.CviPII in random DNA amplification. *Nucleic Acids Res.*, **32**, 6187–6199.
- Kachalova,G.S., Rogulin,E.A., Yunusova,A.K., Artyukh,R.I., Perevyazova,T.A., Matvienko,N.I., Zheleznyaya,L.A. and Bartunik,H.D. (2008) Structural analysis of the heterodimeric type IIS restriction endonuclease R.BspD61 acting as a complex between a monomeric site-specific nickase and a catalytic subunit. *J. Mol. Biol.*, **384**, 489–502.
- Xu,Y., Lunnen,K.D. and Kong,H. (2001) Engineering a nicking endonuclease N.AlwI by domain swapping. *Proc. Natl Acad. Sci. USA*, **98**, 12990–12995.
- Zhang,P., Too,P.H., Samuelson,J.C., Chan,S.H., Vincze,T., Doucette,S., Backstrom,S., Potamouis,K.D., Schramm,T.M., Forrest,D. *et al.* (2010) Engineering BspQI nicking enzymes and application of N.BspQI in DNA labeling and production of single-strand DNA. *Protein expression and purification*, **69**, 226–234.
- Heiter,D.F., Lunnen,K.D. and Wilson,G.G. (2005) Site-specific DNA-nicking mutants of the heterodimeric restriction endonuclease R.BbvCI. *J. Mol. Biol.*, **348**, 631–640.
- Kostiuk,G., Sasnauskas,G., Tamulaitiene,G. and Siksnys,V. (2011) Degenerate sequence recognition by the monomeric restriction enzyme: single mutation converts BcnI into a strand-specific nicking endonuclease. *Nucleic Acids Res.*, **39**, 3744–3753.
- Sanders,K.L., Catto,L.E., Bellamy,S.R. and Halford,S.E. (2009) Targeting individual subunits of the FokI restriction endonuclease to specific DNA strands. *Nucleic Acids Res.*, **37**, 2105–2115.
- Greenstein,D. and Horiuchi,K. (1989) Double-strand cleavage and strand joining by the replication initiator protein of filamentous phage ϕ 1. *J. Biol. Chem.*, **264**, 12627–12632.
- Nash,R.P., Niblock,F.C. and Redinbo,M.R. (2011) Tyrosine partners coordinate DNA nicking by the *Salmonella typhimurium* plasmid pCU1 relaxase enzyme. *FEBS Lett.*, **585**, 1216–1222.
- Chan,S.H., Stoddard,B.L. and Xu,S.Y. (2011) Natural and engineered nicking endonucleases—From cleavage mechanism to engineering of strand-specificity. *Nucleic Acids Res.*, **39**, 1–18.
- Taylor,G.K. and Stoddard,B.L. (2012) Structural, functional and evolutionary relationships between homing endonucleases and proteins from their host organisms. *Nucleic Acids Res.*, **40**, 5189–5200.
- Landthaler,M., Lau,N.C. and Shub,D.A. (2004) Group I intron homing in *Bacillus* phages SPO1 and SP82: a gene conversion event initiated by a nicking homing endonuclease. *J. Bacteriol.*, **186**, 4307–4314.
- Wang,J., Friedman,G., Doyon,Y., Wang,N.S., Li,C.J., Miller,J.C., Hua,K.L., Yan,J.J., Babiarz,J.E., Gregory,P.D. *et al.* (2012) Targeted gene addition to a predetermined site in the human genome using a ZFN-based nicking enzyme. *Genome Res.*, **22**, 1316–1326.

20. Ramirez, C.L., Certo, M.T., Mussolino, C., Goodwin, M.J., Cradick, T.J., McCaffrey, A.P., Cathomen, T., Scharenberg, A.M. and Joung, J.K. (2012) Engineered zinc finger nickases induce homology-directed repair with reduced mutagenic effects. *Nucleic Acids Res.*, **40**, 5560–5568.
21. Kim, E., Kim, S., Kim, D.H., Choi, B.S., Choi, I.Y. and Kim, J.S. (2012) Precision genome engineering with programmable DNA-nicking enzymes. *Genome Res.*, **22**, 1327–1333.
22. McConnell Smith, A., Takeuchi, R., Pellenz, S., Davis, L., Maizels, N., Monnat, R.J. Jr and Stoddard, B.L. (2009) Generation of a nicking enzyme that stimulates site-specific gene conversion from the I-Anil LAGLIDADG homing endonuclease. *Proc. Natl Acad. Sci. USA*, **106**, 5099–5104.
23. Metzger, M.J., McConnell-Smith, A., Stoddard, B.L. and Miller, A.D. (2011) Single-strand nicks induce homologous recombination with less toxicity than double-strand breaks using an AAV vector template. *Nucleic Acids Res.*, **39**, 926–935.
24. Niu, Y., Tenney, K., Li, H. and Gimble, F.S. (2008) Engineering variants of the I-SceI homing endonuclease with strand-specific and site-specific DNA-nicking activity. *J. Mol. Biol.*, **382**, 188–202.
25. Petek, L.M., Russell, D.W. and Miller, D.G. (2010) Frequent endonuclease cleavage at off-target locations in vivo. *Mol. Ther.*, **18**, 983–986.
26. Taylor, G.K., Heiter, D.F., Pietrovski, S. and Stoddard, B.L. (2011) Activity, specificity and structure of I-Bth03051: a representative of a new homing endonuclease family. *Nucleic Acids Res.*, **39**, 9705–9719.
27. Gersbach, C.A., Gaj, T., Gordley, R.M., Mercer, A.C. and Barbas, C.F. 3rd (2011) Targeted plasmid integration into the human genome by an engineered zinc-finger recombinase. *Nucleic Acids Res.*, **39**, 7868–7878.
28. Prorocic, M.M., Wenlong, D., Olorunniji, F.J., Akopian, A., Schloetel, J.G., Hannigan, A., McPherson, A.L. and Stark, W.M. (2011) Zinc-finger recombinase activities in vitro. *Nucleic Acids Res.*, **39**, 9316–9328.
29. Xu, S.Y., Nugent, R.L., Kasamkattil, J., Fomenkov, A., Gupta, Y., Aggarwal, A., Wang, X., Li, Z., Zheng, Y. and Morgan, R. (2012) Characterization of type II and III restriction-modification systems from *Bacillus cereus* strains ATCC 10987 and ATCC 14579. *J. Bacteriol.*, **194**, 49–60.
30. Roy, A., Kucukural, A. and Zhang, Y. (2010) I-TASSER: a unified platform for automated protein structure and function prediction. *Nat. Protoc.*, **5**, 725–738.
31. Emsley, P., Lohkamp, B., Scott, W.G. and Cowtan, K. (2010) Features and development of Coot. *Acta Crystallogr. D Biol. Crystallogr.*, **66**, 486–501.
32. Roberts, R.J., Belfort, M., Bestor, T., Bhagwat, A.S., Bickle, T.A., Bitinaite, J., Blumenthal, R.M., Degtyarev, S., Dryden, D.T., Dybvig, K. et al. (2003) A nomenclature for restriction enzymes, DNA methyltransferases, homing endonucleases and their genes. *Nucleic Acids Res.*, **31**, 1805–1812.
33. Moodley, S., Maxwell, K.L. and Kanelis, V. (2012) The protein gp74 from the bacteriophage HK97 functions as a HNH endonuclease. *Protein Sci.*, **21**, 809–821.
34. Bujnicki, J.M., Radlinska, M. and Rychlewski, L. (2000) Atomic model of the 5-methylcytosine-specific restriction enzyme McrA reveals an atypical zinc finger and structural similarity to betabetaalphaMe endonucleases. *Mol. Microbiol.*, **37**, 1280–1281.
35. Fouts, D.E., Rasko, D.A., Cer, R.Z., Jiang, L., Fedorova, N.B., Shvartsbeyn, A., Vamathevan, J.J., Tallon, L., Althoff, R., Arbogast, T.S. et al. (2006) Sequencing *Bacillus anthracis* typing phages gamma and cherry reveals a common ancestry. *J. Bacteriol.*, **188**, 3402–3408.
36. Bennett-Lovsey, R.M., Herbert, A.D., Sternberg, M.J. and Kelley, L.A. (2008) Exploring the extremes of sequence/structure space with ensemble fold recognition in the program Phyre. *Proteins*, **70**, 611–625.
37. Li, L., Wu, L.P. and Chandrasegaran, S. (1992) Functional domains in FokI restriction endonuclease. *Proc. Natl Acad. Sci. USA*, **89**, 4275–4279.
38. Zhang, P., Bao, Y., Higgins, L. and Xu, S.Y. (2007) Rational design of a chimeric endonuclease targeted to NotI recognition site. *Protein Eng. Des. Sel.*, **20**, 497–504.
39. Sukackaitė, R., Lagunavicius, A., Stankevicius, K., Urbanke, C., Venclovas, C. and Siksnys, V. (2007) Restriction endonuclease BpuJI specific for the 5'-CCCGT sequence is related to the archaeal Holliday junction resolvase family. *Nucleic Acids Res.*, **35**, 2377–2389.
40. Claesson, M.J., Li, Y., Leahy, S., Canchaya, C., van Pijkeren, J.P., Cerdeno-Tarraga, A.M., Parkhill, J., Flynn, S., O'Sullivan, G.C., Collins, J.K. et al. (2006) Multireplicon genome architecture of *Lactobacillus salivarius*. *Proc. Natl Acad. Sci. USA*, **103**, 6718–6723.
41. Durmaz, E., Miller, M.J., Azcarate-Peril, M.A., Toon, S.P. and Klaenhammer, T.R. (2008) Genome sequence and characteristics of Lrml, a prophage from industrial *Lactobacillus rhamnosus* strain M1. *Appl. Environ. Microbiol.*, **74**, 4601–4609.
42. Wang, Y. and Zhang, X. (2008) Characterization of a novel portal protein from deep-sea thermophilic bacteriophage GVE2. *Gene*, **421**, 61–66.
43. Fu, F., Sander, J.D., Maeder, M., Thibodeau-Beganny, S., Joung, J.K., Dobbs, D., Miller, L. and Voytas, D.F. (2009) Zinc Finger Database (ZiFDB): a repository for information on C2H2 zinc fingers and engineered zinc-finger arrays. *Nucleic Acids Res.*, **37**, D279–D283.
44. Rebar, E.J., Greisman, H.A. and Pabo, C.O. (1996) Phage display methods for selecting zinc finger proteins with novel DNA-binding specificities. *Methods Enzymol.*, **267**, 129–149.
45. Joung, J.K., Ramm, E.I. and Pabo, C.O. (2000) A bacterial two-hybrid selection system for studying protein-DNA and protein-protein interactions. *Proc. Natl Acad. Sci. USA*, **97**, 7382–7387.
46. Barbas, C.F. 3rd, Rader, C., Segal, D.J., List, B. and Turner, J.M. (2000) From catalytic asymmetric synthesis to the transcriptional regulation of genes: in vivo and in vitro evolution of proteins. *Adv. Protein Chem.*, **55**, 317–366.
47. Sander, J.D., Zaback, P., Joung, J.K., Voytas, D.F. and Dobbs, D. (2009) An affinity-based scoring scheme for predicting DNA-binding activities of modularly assembled zinc-finger proteins. *Nucleic Acids Res.*, **37**, 506–515.
48. Smith, J., Berg, J.M. and Chandrasegaran, S. (1999) A detailed study of the substrate specificity of a chimeric restriction enzyme. *Nucleic Acids Res.*, **27**, 674–681.
49. Chandrasegaran, S. and Smith, J. (1999) Chimeric restriction enzymes: what is next? *Biol. Chem.*, **380**, 841–848.
50. Wolfe, S.A., Nekludova, L. and Pabo, C.O. (2000) DNA recognition by Cys2His2 zinc finger proteins. *Annu. Rev. Biophys. Biomol. Struct.*, **29**, 183–212.
51. Wright, D.A., Thibodeau-Beganny, S., Sander, J.D., Winfrey, R.J., Hirsh, A.S., Eichinger, M., Fu, F., Porteus, M.H., Dobbs, D., Voytas, D.F. et al. (2006) Standardized reagents and protocols for engineering zinc finger nucleases by modular assembly. *Nat. Protoc.*, **1**, 1637–1652.
52. Carroll, D. (2011) Genome engineering with zinc-finger nucleases. *Genetics*, **188**, 773–782.
53. Pavletich, N.P. and Pabo, C.O. (1991) Zinc finger-DNA recognition: crystal structure of a Zif268-DNA complex at 2.1 Å. *Science*, **252**, 809–817.
54. Huang, H. and Yuan, H.S. (2007) The conserved asparagine in the HNH motif serves an important structural role in metal finger endonucleases. *J. Mol. Biol.*, **368**, 812–821.
55. Kleanthous, C., Kuehlmann, U.C., Pommer, A.J., Ferguson, N., Radford, S.E., Moore, G.R., James, R. and Hemmings, A.M. (1999) Structural and mechanistic basis of immunity toward endonuclease colicins. *Nat. Struct. Biol.*, **6**, 243–252.
56. Kuhlmann, U.C., Moore, G.R., James, R., Kleanthous, C. and Hemmings, A.M. (1999) Structural parsimony in endonuclease active sites: should the number of homing endonuclease families be redefined? *FEBS Lett.*, **463**, 1–2.
57. Shen, B.W., Heiter, D.F., Chan, S.H., Wang, H., Xu, S.Y., Morgan, R.D., Wilson, G.G. and Stoddard, B.L. (2010) Unusual target site disruption by the rare-cutting HNH restriction endonuclease PacI. *Structure*, **18**, 734–743.
58. Sokolowska, M., Czapinska, H. and Bochtler, M. (2009) Crystal structure of the beta beta alpha-Me type II restriction endonuclease Hpy99I with target DNA. *Nucleic Acids Res.*, **37**, 3799–3810.

59. Kelley, L.A. and Sternberg, M.J. (2009) Protein structure prediction on the Web: a case study using the Phyre server. *Nat. Protoc.*, **4**, 363–371.
60. Handel, E.M., Alwin, S. and Cathomen, T. (2009) Expanding or restricting the target site repertoire of zinc-finger nucleases: the inter-domain linker as a major determinant of target site selectivity. *Mol. Ther.*, **17**, 104–111.
61. Veith, T., Martin, R., Wurm, J.P., Weis, B.L., Duchardt-Ferner, E., Saffertal, C., Hennig, R., Mirus, O., Bohnsack, M.T., Wohnert, J. *et al.* (2012) Structural and functional analysis of the archaeal endonuclease Nob1. *Nucleic Acids Res.*, **40**, 3259–3274.
62. Elsby, L.M. and Roberts, S.G. (2008) Interaction of the TFIIB zinc ribbon with RNA polymerase II. *Biochem. Soc. Trans.*, **36**, 595–598.
63. Vanamee, E.S., Hsieh, P., Zhu, Z., Yates, D., Garman, E., Xu, S. and Aggarwal, A.K. (2003) Glucocorticoid receptor-like Zn(Cys)₄ motifs in BslI restriction endonuclease. *J. Mol. Biol.*, **334**, 595–603.
64. Saravanan, M., Vasu, K., Ghosh, S. and Nagaraja, V. (2007) Dual role for Zn²⁺ in maintaining structural integrity and inducing DNA sequence specificity in a promiscuous endonuclease. *J. Biol. Chem.*, **282**, 32320–32326.
65. Grishin, N.V. (2000) C-terminal domains of Escherichia coli topoisomerase I belong to the zinc-ribbon superfamily. *J. Molecular Biol.*, **299**, 1165–1177.
66. Moodley, S. (2010) Biochemical investigation of the bacteriophage protein HK97 gp74. *M.S. Thesis. University of Toronto*, 1–102.
67. Chan, S.H., Opitz, L., Higgins, L., O’Loane, D. and Xu, S.Y. Cofactor requirement of HpyAV restriction endonuclease. *PLoS One*, **5**, e9071.
68. Liu, G., Ou, H.Y., Wang, T., Li, L., Tan, H., Zhou, X., Rajakumar, K., Deng, Z. and He, X. (2010) Cleavage of phosphorothioated DNA and methylated DNA by the type IV restriction endonuclease ScoMcrA. *PLoS Genet.*, **6**, e1001253.
69. Christian, M., Cermak, T., Doyle, E.L., Schmidt, C., Zhang, F., Hummel, A., Bogdanove, A.J. and Voytas, D.F. (2010) Targeting DNA double-strand breaks with TAL effector nucleases. *Genetics*, **186**, 757–761.
70. Morbitzer, R., Elsaesser, J., Hausner, J. and Lahaye, T. (2011) Assembly of custom TALE-type DNA binding domains by modular cloning. *Nucleic Acids Res.*, **39**, 5790–5799.
71. Li, T., Huang, S., Jiang, W.Z., Wright, D., Spalding, M.H., Weeks, D.P. and Yang, B. (2011) TAL nucleases (TALNs): hybrid proteins composed of TAL effectors and FokI DNA-cleavage domain. *Nucleic Acids Res.*, **39**, 359–372.
72. Sanjana, N.E., Cong, L., Zhou, Y., Cunniff, M.M., Feng, G. and Zhang, F. (2012) A transcription activator-like effector toolbox for genome engineering. *Nat. Protoc.*, **7**, 171–192.
73. Mahfouz, M.M., Li, L., Shamimuzzaman, M., Wibowo, A., Fang, X. and Zhu, J.K. (2011) De novo-engineered transcription activator-like effector (TALE) hybrid nuclease with novel DNA binding specificity creates double-strand breaks. *Proc. Natl Acad. Sci. USA*, **108**, 2623–2628.
74. Miller, J.C., Tan, S., Qiao, G., Barlow, K.A., Wang, J., Xia, D.F., Meng, X., Paschon, D.E., Leung, E., Hinkley, S.J. *et al.* (2011) A TALE nuclease architecture for efficient genome editing. *Nat. Biotechnol.*, **29**, 143–148.
75. Reyon, D., Tsai, S.Q., Khayter, C., Foden, J.A., Sander, J.D. and Joung, J.K. (2012) FLASH assembly of TALENs for high-throughput genome editing. *Nat. Biotechnol.*, **30**, 460–465.
76. Briggs, A.W., Rios, X., Chari, R., Yang, L., Zhang, F., Mali, P. and Church, G.M. (2012) Iterative capped assembly: rapid and scalable synthesis of repeat-module DNA such as TAL effectors from individual monomers. *Nucleic Acids Res.*, **40**, e117.
77. Chu, S.W., Noyes, M.B., Christensen, R.G., Pierce, B.G., Zhu, L.J., Weng, Z., Stormo, G.D. and Wolfe, S.A. (2012) Exploring the DNA-recognition potential of homeodomains. *Genome Res.*, **22**, 1889–1898.
78. Fomenkov, A., Too, P.H., Chan, S.H., Vaisvila, R., Cantin, B.A., Mazzola, L., Tam, V. and Xu, S.Y. (2008) Targeting DNA 5mCpG sites with chimeric endonucleases. *Anal. Biochem.*, **381**, 135–141.
79. Wilson, G.W. and Edgell, D.R. (2009) Phage T4 mobE promotes trans homing of the defunct homing endonuclease I-TevIII. *Nucleic Acids Res.*, **37**, 7110–7123.